Available online at www.sciencedirect.com
SCIENCE DIRECT®
ELSEVIER
Materials Science in Semiconductor Processing 7 (2004) 289–294
MATERIALS SCIENCE IN SEMICONDUCTOR PROCESSING

Depth profiled porosity and microstructure evolution studied by positron annihilation and Raman spectroscopy in SiOCH low-κ films

C. Macchi, G. Mariotto, G.P. Karwasz, A. Zecca, M. Bettonte, R.S. Brusa*

Dipartimento di Fisica, Università di Trento and INFM, I-38050 Povo (TN), Italy

Available online 20 October 2004

Abstract

The 3γ annihilation of ortho-positronium and the Doppler broadening of the positron annihilation line have been measured by implanting low-energy positrons in low dielectric constant (low-κ) SiOCH films. Positron techniques were used to gather information about the porosity while Raman scattering was employed to study the microstructure of the films. The evolution of both the film porosity and microstructure was monitored as a function of the thermal treatments in the 400–900 °C temperature range. The films were produced by plasma enhanced chemical vapor deposition (PECVD), and after annealing in N_2 atmosphere at 400 °C they were treated in N_2 + He plasma. The treatment in the N_2 plasma was found to seal the pores within a surface layer 45 nm thick. The minimum free volume of the pores in the as-produced samples has been estimated. The chemical environment of the pores probed by positrons was found to be stable up to 600 °C thermal treatment. At 700–900 °C annealing temperature a reduction of the hydrogen content and a change in the chemical environment of the pores has been observed. Raman spectroscopy indicates the formation of carbon inclusions within the film treated at temperatures equal to and higher than 500 °C.

Keywords: SiOCH films; Positron annihilation spectroscopy; Vibrational spectroscopy; Raman scattering; Porosity; Carbon inclusions

1. Introduction

As pointed out in the *Interconnection* chapter of the 2003 *International Technology Roadmap for Semiconductors* [1] one of the most difficult challenges to reach the near term technology node of $\geqslant$ 45 nm through 2009 is the realization and integration of very low dielectric constant materials ($\kappa < 2.1$). The introduction of copper for wiring system to meet the need of high speed requires the development and the integration of insulating materials with low-κ values in substitution of silicon oxide. The demand is due to the necessity to decrease the capacitance between wires to lower the delay in signal transmission and the power consumption. Low-κ materials are expected to be already in use for the 90 nm technology node, but still many related aspects are challenging. The first open problem is the best choice of the porous material according to its properties: many materials are being investigated and the two major classes are the spin-on (silsesquioxane-based materials) and plasma enhanced chemical vapor deposition (PECVD) deposited materials (silica-based materials) [2]. For the integration of low-κ materials the primary need is to solve the adhesion failure between barrier or capping materials and the dielectric during planarization. Low-κ SiOCH films can be easily capped by

*Corresponding author. Tel.: ++39 0461 881552; fax: ++39 0461 881696.
E-mail address: brusa@science.unitn.it (R.S. Brusa).

1369-8001/$ - see front matter © 2004 Elsevier Ltd. All rights reserved.
doi:10.1016/j.mssp.2004.09.093

treatment in N_2 plasma at moderate temperature, at which the film still retains a good stability.

In this paper we have studied the structural stability of SiOCH material, deposited by PECVD as a function of thermal treatments. On the deposited film a capping was obtained by a treatment in N_2 plasma with the aim to improve the adhesion of further layers. We have applied two complementary techniques: the depth profiling with positron annihilation spectroscopy (DP-PAS), which is very sensitive to open volume defects and porosity [3–5], and Raman spectroscopy, which is particularly suitable to reveal the formation of nano-precipitates or nano-structures within the amorphous matrix of films. Chemical bond investigation of the same material with the Fourier transform infrared (FTIR) spectroscopy can be found elsewhere [6].

DP-PAS is one among the few analytical techniques available to characterize the porosity in thin dielectric films [7]. In particular with DP-PAS it is possible to obtain information on distribution, sizes and interconnectivity of the pores. DP-PAS, small-angle neutron scattering (SANS) and small-angle X-ray scattering (SAXS) combined with X-ray reflectivity (XRR) and ellipsometric porosimetry (EP) have been applied to characterize the porosity in the same set of samples (MSQ and HSQ films). The results of different techniques were compared and their potentiality and limitation discussed [2]. DP-PAS, SAXS with XRR and EP techniques have been also used to study the same set of SiOCH films [8]. The results obtained from the above-mentioned techniques were found to be in good agreement if we take into account that these techniques are based on different physical–chemical principles and that the DP-PAS data must be analyzed with appropriate models in order to extract information on pores structure.

Some recent papers deal with structural and porosity characterization of SiOCH materials deposited by PECVD, but starting from different precursors [8–11]. It seems that the value of the dielectric constant in SiOCH, with $\kappa < 2.8$, is mainly determined by the degree of porosity and not from the composition of the material [8]. An important aspect under investigation within this work is the stability of the pore structure with thermal treatments.

2. Experimental

SiOCH films were deposited by PECVD on Si (p-100) substrates using trimethylsilane + O_3 at 120 °C and a pressure of 100 Torr. The wafer with the deposited film was thermally treated in atmospheric pressure of N_2 at 400 °C (30 min). The wafer was further treated in a N_2 + He plasma (1.5 Torr) at 700 W rf power for 120 s at 400 °C with the aim to generate a nitride capping layer on the film. After these preliminary treatments, a series of samples was thermally treated for 30 min in vacuum at fixed temperatures in the range from 400 to 900 °C. In a previous work [11], we have studied by DP-PAS SiOCH films prepared with the same procedure but deposited at 480 °C. In that paper we also focused on natural aging of the material in air and artificial aging in controlled atmospheres of H_2, O_2, H_2O.

The thickness of the as-deposited and treated film, as measured by cross-section microscopy, was found to be 310 nm, while its density, measured by weighting before and after deposition and treatments was found to be 1.25 g cm^{-3}. The dielectric constant κ was 2.95 as determined by electrical measurements, and the composition of the as-produced film determined by Rutherford backscattering spectroscopy (RBS) and elastic recoil detection analysis (ERDA) measurements was $SiO_{1.5}C_{1.2}H_3$. It is worth noting that the thermal treatments up to 600 °C do not produce appreciable change in the composition of the film. On the contrary, the thermal treatment at 700 °C reduces the hydrogen content to one-half of the initial content, and at 800 and 900 °C the H content is about one-fourth.

DP-PAS measurements have been obtained with an electrostatic slow positron beam tunable in the 80 eV–26 keV energy (E) ranges [12]. These positron implantation energies correspond to a probed film thickness ranging from 0.6 nm to a few microns. The positron beam was coupled to a high-purity germanium detector with a resolution of 1.2 keV at 511 keV. At each positron implantation energy the 511 keV gamma line was acquired with a microspectrum method and stabilized by a software procedure [13].

Positrons injected in a solid reach thermal energies in few picoseconds, then after a diffusion path they are efficiently trapped in open structures where present and there they annihilate with an electron. The high specific trapping rate of positrons for open volumes makes this particle a very efficient non-destructive probe for characterizing open volume defects from single vacancies up to voids and porosities. The annihilation characteristics are determined by the local electronic environment of the annihilation site. In the present work we have used Doppler broadening spectroscopy (DBS) 2–3 gamma ratios of positronium (3γ-PAS) and two complementary DP-PAS techniques, to extract the physical and chemical information concerning the annihilation site. With these techniques, the 511 keV annihilation line is analyzed through characteristic parameters [3,4] to extract information from the transferred momentum of positron–electron pairs.

3γ-PAS is based on the positron possibility of forming positronium (Ps), the bound state with an electron, in insulator materials. When pores are present in the material, positrons are favorably trapped there and form Ps and Ps in a pore loses energy by means of inelastic

collisions with the walls and is not able to re-enter the solid [14]. The Ps annihilation characteristics depend on the pore size and on the chemical composition of the pore surfaces [7,14,15]. When formed, Ps is the ideal probe for porosity with pore size > 1 nm. Ps is formed in two different states: para-positronium *p*-Ps (↑↓ anti-parallel spin configuration, formation probability 1/4), ortho-positronium *o*-Ps (↑↑ parallel spin configuration, formation probability 3/4). *p*-Ps annihilates mainly into two γ-rays by self-annihilation, while *o*-Ps trapped into a void can annihilate into three γ-rays by self-annihilation with the bound electron or into two γ-rays with an electron of the void surface (pick-off annihilation). The pick-off annihilation rate (λ_{po}) is related to the void size of the pores because of its dependence on the electron density in the annihilation site [16–18]. The 3γ energy (E_γ) distribution of *o*-Ps decay ranges from zero to 511 keV, while the *o*-Ps pick-off and *p*-Ps decay are confined around 511 keV. The 3γ vs. 2γ ratio is evaluated with the *R* parameter, here defined as the ratio of the counts in the $410\,\text{keV} < E_\gamma < 500\,\text{keV}$ energy range and the counts in the peak ($|511–E_\gamma| \leqslant 4.25\,\text{keV}$). An increase in the 3γ annihilation contributes to the increase of *R*: such an increase (due to a decrease in the pick-off annihilation rate) indicates the presence of larger pores in the samples, in the hypothesis of no chemical variation on the walls of the pores. The scale of *R* can be calibrated [19,20]. For details on the present calibration see Ref. [11]. The R_n parameter obtained in this way is the fraction of positron forming Ps (F_{Ps}) times the 3γ annihilation probability [11,21]

$$R_n = F_{Ps}\,\frac{\lambda_{3\gamma}}{\lambda_{3\gamma}+\lambda_{po}}, \tag{1}$$

where $\lambda_{3\gamma} = (142.1\,\text{ns})^{-1}$ is the *o*-Ps annihilation rate in vacuum and λ_{po} the pick-off annihilation rate.

DBS measurements have been utilized to extract information about the distribution of open volumes in the different layers of the samples and about the chemical environment on the wall of the pores. With DBS the 511 keV annihilation peak is usually characterized by the two parameters *S* and *W* that are normalized to the Si bulk value S_b ($S_n = S/S_b$) and W_b ($W_n = W/W_b$) of the substrate. The S_n parameter, defined as the ratio between the counts in a central area of the peak ($|511-E_\gamma| \leqslant 0.85\,\text{keV}$) and the counts in the total area of the peak ($|511-E_\gamma| \leqslant 4.25\,\text{keV}$), represents the fraction of positron annihilating with low-momentum electrons. The S_n value increases when positrons annihilate in open volume defects and/or when Ps annihilate by 2γ or by pick-off. The W_n parameter, defined as the ratio between the counts in the wing regions of the peak ($1.6\,\text{keV} \leqslant |511-E_\gamma| \leqslant 4\,\text{keV}$) and the counts in the total area of the peak, represents the fraction of positron annihilating with high-momentum electrons. Simultaneous analysis of S_n and W_n values with the $S_n(E)$ vs. $W_n(E)$ curves provides information about the chemical species at the annihilation site [14,22].

Micro-Raman spectra were excited at room temperature in backscattering geometry by the 488.0 nm line of an Ar^+ ion laser. A high Numerical Aperture (N.A. = 0.95) 100× objective was used both to inject and focus the laser beam onto the film surface and to collect the scattered light. The power density of laser beam at the film surface of the order of $10^5\,\text{W cm}^{-2}$ was kept with the purpose of avoiding unwanted heating effects. The radiation scattered from the film as well as from the underlying Si substrate was filtered by a double monochromator (Jobin–Yvon, model Ramanor HG2-S, 1 m focal length), equipped with holographic gratings ($2000\,\text{groves mm}^{-1}$). The signal was detected by a standard photon–counting system, thermoelectrically cooled at about –35 °C. Unpolarized spectra were carried out in the region between 400 and $1800\,\text{cm}^{-1}$ with the aim to detect the scattering from carbon inclusions, if present as separated phase within the SiCOH layer.

3. Results and discussion

The open volume structure of the studied SiOCH samples can be described by the analysis of the S_n vs. *E* curves presented in Fig. 1(a). The upper scale in Fig. 1(a) reports the mean positron implantation depth evaluated according to the relation $z = (40/\rho)\,E^{1.6}$, with *z* in nm when the density ρ and the positron implantation energy *E* are expressed in g cm^{-3} and keV, respectively. The scale was evaluated with the density of the as-produced sample. The data fitting is obtained by means of a procedure (VEPFIT program [23]) based on the solution of the stationary positron diffusion equation. The as-prepared sample is found to be composed of four layers. The first one extends up to 45 nm, has a constant low S_n value and is associated to the SiOCH part of the film, of interest in N_2 + He plasma treatment. The second layer, from 45 to 310 nm, is the SiOCH film; here, the S_n parameter reaches a very high S_n value (> 1.14), strong indication of the presence of large voids. These large voids, in the following, will be denoted as pores because of their dimension (see below). The third layer is a very thin (2 nm) interface between the SiOCH film and the Si substrate due to the existence of a native silicon oxide on the wafer surface before the film deposition. Finally, the S_n curve decreases towards the S_n silicon bulk value.

The analysis points out that the treatment in N_2 plasma produces the sealing of the open SiOCH structure forming a capping layer that extends several nanometers in depth below the surface. The S_n value in this capping layer does not change with thermal

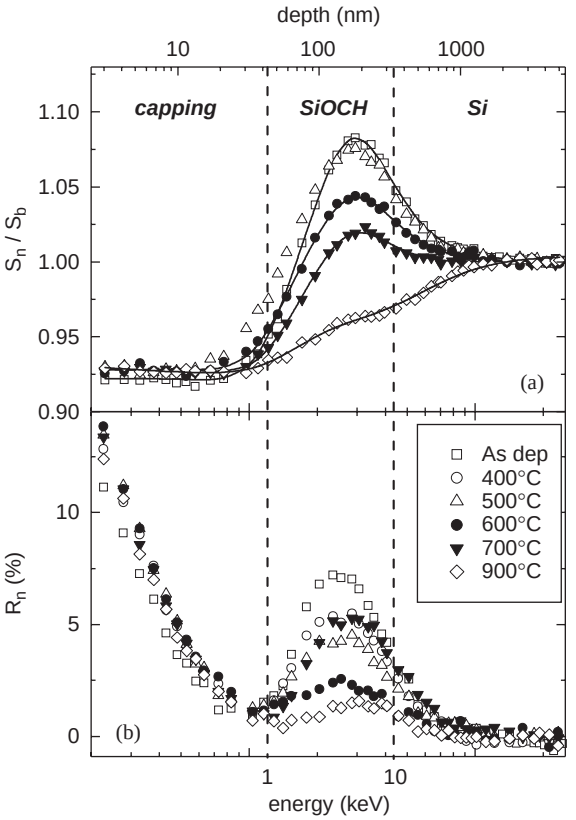

Fig. 1. (a) S_n parameter and (b) R_n parameter as a function of positron implantation energy and as a function of depth (upper axis).

treatment up to 900 °C, showing that the structure of the capping is very stable.

The S_n value in the SiOCH film does not change with thermal treatment up to 500 °C. A small decrease of S_n is observed at 600 °C, and a more perceptible decrease at 700 °C. The stronger effect is at 800 and 900 °C, where the S_n parameter reaches 0.96. This decrease is associated with a decrease of the volume of pores [5,11,21].

The detection of the *o*-Ps 3γ decay, reflected in the R_n parameter (Fig. 1(b)), clearly shows the presence of pores in the SiOCH film. In the capping layer, the rise of the R_n parameter from about zero at 45 nm to a high value at the surface is only due to the fact that positrons after diffusing to the surface have enough energy to pick an electron and to escape in the vacuum as Ps atoms. From 45 nm to the film/substrate interface, R_n increases reaching its maximum value of about 7% around 140 nm depth, then the 3γ decay probability tends towards zero in the bulk silicon. A lower bound for the sizes of the pores can be estimated by Eq. (1) assuming that implanted and diffused positrons in the SiOCH film have 100% probability (F_{Ps}) to form Ps, and remembering that λ_{po} can be directly related to the pore size with models [16–18]. We obtain that the diameter of pores in the present as-prepared SiOCH samples is larger than 1.3–1.4 nm, assuming a spherical shape. From 400 °C there is a decrease in the R_n values. This decrease is stronger at 600 °C. An increase, probably due to a chemical modification of the pore walls, is observed at 700 °C. Finally, at 800 and 900 °C, R_n decreases drastically, pointing out a strong decrease in the porosity of the samples.

3γ-PAS technique allows determining if pores are interconnected by studying the out diffusion of formed Ps: if the pores are interconnected, Ps can in fact find a path through a channel of connected pores toward the vacuum surface [15]. In our samples, due to the capping layer that seals the surface, it is not possible to have any indication about pore connectivity. Experimentally, the porosity is seen as closed.

Micro-Raman spectra are shown in Fig. 2. Raman signal of as-produced film, the spectrum of which is not shown in the figure, originates entirely from the Si substrate, and consists of the c-Si peak at 520 cm^{-1}, with no appreciable contribution from the SiCOH layer, due to both the scarce Raman scattering efficiency of carbon-doped silicon dioxide and the reduced thickness of the film. Likewise, no Raman scattering from the SiCOH material is observed in the spectra of samples thermally treated up to 500 °C. In the spectra of the sample treated at 500 °C, two weak but clearly shaped bands appear in the region between 1200 and 1700 cm^{-1}. They are typical of sp^2-hybridized carbon forms. The first band (D peak) is centered at about 1350 cm^{-1}. The second band (G peak) is centered at about 1580 cm^{-1},

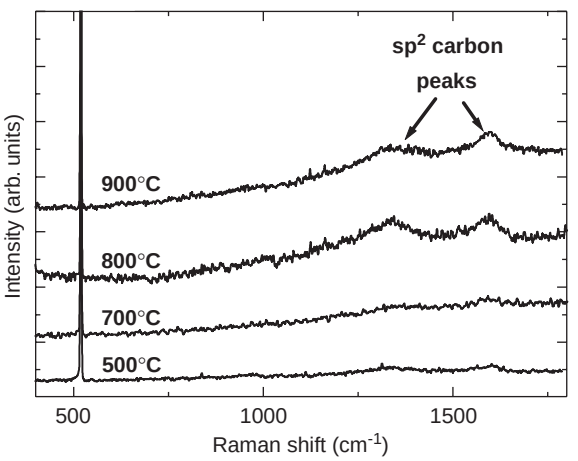

Fig. 2. Room temperature micro-Raman spectra of samples after annealing in vacuum at 500, 700, 800 and 900 °C.

the position of which is typical of disordered graphite. Therefore, the D and G bands have to be related to an appreciable formation of sp^2 carbon clusters in the SiOCH film. These two bands occur in the same position and show similar relative intensities in the spectra of the samples thermally treated at 700 °C. Finally, in samples treated at 800 and 900 °C they still peak at the same energy but their intensity is relatively stronger, thus suggesting that an important structural rearrangement, with the formation of a remarkable amount of sp^2-carbon inclusions has occurred in film annealed at these temperatures.

The chemical environment, probed by positron annihilating in the pores, changes as the samples are thermally treated at temperatures higher than 500 °C. As the hydrogen content diminishes with the thermal treatments, the S_n values decrease and the W_n values increase (see Fig. 3). The couple of values S_n–W_n equal to 0.96–1.2, reached in the samples treated at 800 and 900 °C, corresponds to annihilation in proximity of oxygen and carbon [5,11].

Summarizing the above results we can draw a picture of the microstructural evolution of the SiOCH film under thermal treatments. SiOCH is a silica-based material in which Si–O bonds are partially substituted by -CH_3 groups. The structure is that of long chains with different degrees of cross-linking [2,9]. In our material, the formed pores have sizes bigger than 1.3 nm in diameter and, probably, their walls are mainly decorated by hydrogen. This structure is quite stable with thermal treatments up to 500 °C, where the early step of carbon agglomeration occurs. At 600 °C the small decrease of the S_n values and of 3γ annihilation can be probably associated to the release of weakly bonded H (Si–H bonds break starting from 400 °C): the effects on S_n and

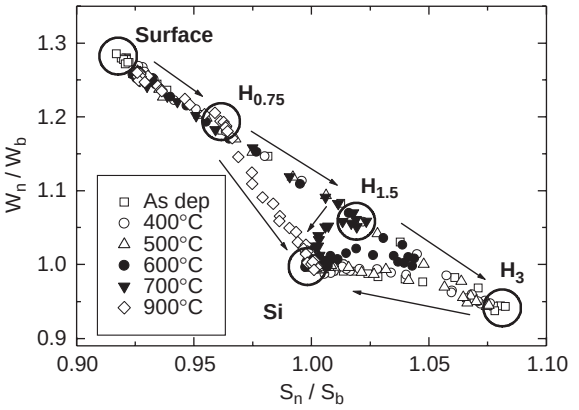

Fig. 3. $S_n(E)$–$W_n(E)$ plot for the as-produced and annealed SiOCH samples. Arrows indicate increasing depth. S_n–W_n values, characterizing the chemical environment probed by positrons in the pore, are encircled and denoted by the hydrogen content of samples.

R_n is consistent with an increase of positron annihilation with O and C electrons. The out diffusion of 50% and 75% of H at 700 and 800–900 °C, respectively, is due to the strong C–H bond break which also leaves free C-bonds at the walls of the pores. These carbon atoms can then give rise to C–C bonds forming the carbon inclusions observed by the Raman spectroscopy. At temperature higher than 600 °C, Si–C bonds are also expected to be unstable producing free C atoms that can contribute to the formation of carbon inclusions. The consequence of the above two effects is that porosity of treated samples changes both in dimensions and in chemical structure. Many pores can reduce their size, or even disappear, due to the C–C connection and C agglomeration; the remaining pores have walls more rich in O and C due to the H loss. This view is consistent with 3γ-PAS and DBS measurements [Figs. 1 and 3], as described. FTIR measurements [6] show that a signal due to Si–C bonds also remains after thermal treatments: this finding does not exclude that the C inclusion maintains some degree of connection with the matrix.

4. Conclusions

The microstructural evolution of SiOCH films as a function of thermal treatments was studied by two complementary non-destructive techniques (Raman spectroscopy and PAS). It was possible to give a description of the change in porosity (size and chemical structure) associated to the release of H and to the presence of carbon inclusions within the composite matrix of the film. The formation of carbon agglomerates and the decrease of pore concentration as a function of thermal treatments may cause a shrinkage of the film structure. It must be very interesting to gain experimental evidence by direct measurements.

References

[1] International Technology Roadmap for Semiconductors, 2003.
[2] Maex K, Baklanov MR, Shamiryan D, Iacopi F, Brongersma SH, Yanovitskaya ZS. Appl Phys 2003;93:8793.
[3] Schultz PJ, Lynn KG. Rev Mod Phys 1988;60:701.
[4] Dupasquier A, Mills Jr AP, editors. Positron spectroscopy of solids. IOS 1995.
[5] Asoka-Kumar P, Lynn KG, Welch DO. J Appl Phys 1994;76:4935.
[6] Das G, Mariotto G, Quaranta A. Mater Sci, these proceedings, Paper Number 1410.
[7] Gidley DW, Lynn KG, Petkov MP, Weber MH, Sun JN, Yee AF. In: Surko CM, Gianturco FA editors. New directions in antimatter chemistry and physics. Dordrecht: Kluwer Academic Publishers; 2001. p. 151–71.

[8] Grill A, Pantel V, Rodbell KP, Huang E, Baklanov MR, Mogilnikov KP, Toney M, Kim H-C. J Appl Phys 2003;94:3427.
[9] Grill A, Neumayer D. J Appl Phys 2003;94:6697.
[10] Sil Yang C, Yu Y-H, Lee K-M, Lee H-J, Choi CK. Thin Solid Films 2003;435:165.
[11] Brusa RS, Spagolla M, Karwasz GP, Zecca A, Ottaviani G, Corni F, Bacchetta M, Carollo E. J Appl Phys 2004;95:2348.
[12] Zecca A, Bettonte M, Paridaens J, Karwasz GP, Brusa RS. Meas Sci Technol 1998;9:1.
[13] Brusa RS, Karwasz GP, Tiengo N, Zecca A, Corni F, Tonini R, Ottaviani G. Phys Rev B 2000;61:10154.
[14] Petkov MP, Weber MH, Lynn KG, Rodbell KP, Cohen SA. J Appl Phys 1999;86:3104.
[15] Petkov MP, Wang CL, Weber MH, Lynn KG, Rodbell KP. J Phys Chem B 2003;107:2725.
[16] Eldrup M. In: Coleman PG, Sharma SC, Diana LM editors. Positron annihilation. Amsterdam: North-Holland; 1982. p. 753.
[17] Nakanishi H, Jean YC. In: Schrader DM, Jean YC editors. Positron and positronium chemistry. Elsevier: Amsterdam; 1988.
[18] Gidley DW, Frieze WE, Dull TL, Sun J, Yee AF, Nguyen CV, Yoon DY. Appl Phys Lett 2000;76:1282.
[19] Mills Jr AP. Phys Rev Lett 1978;41:1828.
[20] Soininen E, Schwab A, Lynn KG. Phys Rev B 1991;43:10051.
[21] Brusa RS, Karwasz GP, Mariotto G, Zecca A, Ferragut R, Folegati P, Dupasquier A, Ottaviani G, Tonini R. J Appl Phys 2003;94:7483.
[22] Clement M, de Nijs JMM, Balk P, Shut H, van Veen A. J Appl Phys 1996;79:9029.
[23] van Veen A, Schut H, de Vries J, Hakvoort RA, Ijpma MR. AIP Conf Proc 1990;218:171.